Structural Eng./Earthquake Eng., JSCE, Vol. 17, No. 2, 225s－240s, 2000 October
(J. Struct. Mech. Earthquake Eng., JSCE, No. 661/ I－53)

SOLUTION OF FINITE-DISPLACEMENT SMALL-STRAIN ELASTICITY PROBLEMS BY REMOVAL OF RIGID BODY DISPLACEMENTS

Fumio NISHINO[1], Sujan MALLA[2] and Takamasa SAKURAI[3]

[1]Fellow of JSCE, Ph.D., Professor, National Graduate Institute for Policy Studies, Tokyo 162-8677, Japan
[2]D. Eng., Structural Engineering Expert, Electrowatt Engineering Ltd., CH-8037 Zurich, Switzerland
[3]Mem. of JSCE, D.Eng., Professor, Dept. of Civil Engineering, Toyota College of Technology, Toyota-shi 471-8525, Japan

If rigid body displacements are properly separated from a finite-displacement small-strain problem, the remaining deformation is within the scope of the small displacement theory. For this purpose, the rigid body displacement of each sufficiently small subdomain of an elastic body must be removed independently from other subdomains before the actual deformation occurs. This paper presents a rigorous and straightforward theoretical formulation for a numerical solution procedure based on this concept. The simplicity of the formulation is due to the fact that it is developed for a general three-dimensional solid rather than structural elements as in the past works.

Key Words: *finite displacement problems, geometric stiffness matrix, finite rotations*

1. INTRODUCTION

Many procedures based on the total and updated Lagrangian descriptions have been proposed to obtain numerical solutions of elastic finite-displacement small-strain problems[1)-6)]. It is often claimed that a proposed method gives exact solutions of finite displacement problems without any theoretically convincing explanation. The fact that many procedures have been presented to solve these problems indicates itself that there is a need for a clearer understanding of the treatment of such problems.

It is well-known that, in the geometrically nonlinear small-strain problems, displacements can be decomposed into large rigid body components and relatively small deformation components[7)-9)]. This paper aims to show that even the small displacement theory is sufficient in each of the subdomains into which a body is divided, if the rigid body displacement is separated. The geometric nonlinearity can be fully accounted for by the transformation matrix, which is a function of the rigid body displacement. Even the use of the geometric stiffness matrix is not necessary, provided that strains are small and the numerical solution procedure converges. This fact has not been clearly reported in the literature, but the geometric stiffness matrix is generally included in the discretized analysis of geometrically nonlinear problems as a necessity. Another related objective of this paper is to show that the solutions obtained by the proposed approach are the exact solutions of the finite-displacement small-strain problems. A theoretically rigorous and straightforward formulation of the approach is provided for a linear elastic solid body. It is additionally aimed to show that numerous complex formulations developed in the past are in fact not necessary to solve the finite-displacement small-strain problems.

The idea of removing the rigid body displacement used in the proposed formulation is similar to that of the co-rotational formulations[9)-11)]. The latter formulations, however, are based only on engineering judgement and are lacking in theoretical background. Because of this, the possibility of solving the problem by neglecting the higher order terms in the governing equations is not recognized. The co-rotational procedure has also been confused with the updated Lagrangian formulation in the past[9), 12)].

The fact that finite rotations do not follow the normal tensorial transformation rules causes difficulty in the normal discretized formulation of governing equations of structures when finite displacements have to be considered. An attempt was made to treat them by introducing the concept of a rotation vector[13)]. However, the appli-

cability of this concept was limited to small rotations only[8]. The concept of the rotation vector was later extended rigorously to be able to deal with finite rotations[8]. The basic discretized equation was derived for structural elements under a number of assumptions in Reference 8. The resulting rotation vector, however, differed from the separately developed rigorous rotation vector. The former quantity was replaced with the latter without providing any theoretical explanation[8].

Considering an elastic body consisting of sufficiently small arbitrary subdomains, each subdomain is subjected to a rigid body displacement independent of the other subdomains. Then, body and surface loads as well as internal and external boundary conditions are imposed bringing the body to its final equilibrium position. The concept of subdomains is inherent in the finite element method and the scheme for the removal of the rigid body displacements can be easily incorporated in its framework.

The material coordinates of all points are defined in the global coordinate system in the original state. However, a local coordinate system can always be defined for each subdomain in the configuration after the rigid body displacement in such a way that the coordinates of each point remain numerically identical to the global material coordinates in the original configuration. As such local coordinates are used to identify the displacement of that point causing deformation in the body, the approach discussed in this paper for the study of the finite-displacement small-strain problems is regarded as a total Lagrangian approach.

2. SEPARATION OF RIGID BODY DISPLACEMENTS

Consider a three-dimensional elastic body undergoing finite displacements but with the deformation remaining within the range of small strains. To analyze the body, the Lagrangian global Cartesian coordinates $\mathbf{x} = \{x_i\} = \{x_1, x_2, x_3\}$ of a material point are defined in the initial loading-free state. The corresponding global orthogonal unit base vectors are denoted by $\{\mathbf{i}_i\} = \{\mathbf{i}_1, \mathbf{i}_2, \mathbf{i}_3\}$. Using the summation convention, the displacement vector of a point $\mathbf{x}$ can be expressed as $\mathbf{u}(\mathbf{x}) = u_i(\mathbf{x})\,\mathbf{i}_i$. The position vector of the same point after the displacement is

$$\mathbf{R}(\mathbf{x}) = \{x_i + u_i(\mathbf{x})\}\mathbf{i}_i \tag{1}$$

where the range of the index i is 1 to 3 in a three-dimensional problem.

The base vectors $\{\mathbf{G}_i\} = \{\mathbf{G}_1, \mathbf{G}_2, \mathbf{G}_3\}$ at a material point $\mathbf{x}$ in an equilibrium position, using the total Lagrangian description, are then obtained by differentiating the position vector $\mathbf{R}(\mathbf{x})$ with respect to the Cartesian coordinates x_i defined in the initial loading-free state as

$$\mathbf{G}_i(x) \equiv \mathbf{R}_{,i}(\mathbf{x}) = \{\delta_{ji} + u_{j,i}(\mathbf{x})\}\,\mathbf{i}_j \tag{2}$$

where δ_{ij} = Kronecker's delta and $(\ )_{,i} = \partial(\ )/\partial x_i$. The Green's strain tensor is defined in terms of the base vectors $\mathbf{i}_i$ and $\mathbf{G}_i$, and, in view of Eq. (2), can be further expressed in terms of the displacement vector, as

$$\begin{aligned} e_{ij} &\equiv \frac{1}{2}(\mathbf{G}_i.\mathbf{G}_j - \mathbf{i}_i.\mathbf{i}_j) \\ &= \frac{1}{2}(u_{i,j} + u_{j,i} + u_{k,i}\,u_{k,j}) \end{aligned} \tag{3}$$

Since this study is limited to small strain problems only, the following relationship holds

$$|e| \approx |e_{ij}| << 1 \tag{4}$$

where e = small non-dimensional quantity representing all the components of the strain tensor after finite displacements.

When the displacements are finite, the base vectors $\mathbf{G}_i$ may be significantly different from $\mathbf{i}_i$. However, in view of Eqs. (3) and (4), the metric tensor $\mathbf{G}_i.\mathbf{G}_j = G_{ij}$ after finite displacements remains close to the metric tensor $\mathbf{i}_i.\mathbf{i}_j = \delta_{ij}$ of the initial state with a difference of the order of small strains, i.e.,

$$\mathbf{G}_i.\mathbf{G}_j = \mathbf{i}_i.\mathbf{i}_j + O(e) \tag{5}$$

where $O(\ )$ = Landau's notation denoting a quantity of the order of the term inside the brackets. Equation (5) indicates that the base vectors $\mathbf{G}_i$ in the final equilibrium configuration are no longer orthogonal unit vectors. However, the deviations from unit lengths and orthogonality conditions are of the order of small strains.

Let us divide the whole domain of the body into M arbitrary subdomains $\{V_{(m)}, m = 1, 2, \ldots, M\}$. The base vectors at an arbitrarily selected point O in each subdomain

$V_{(m)}$ in the final equilibrium state are denoted by $\mathbf{G}_i^o$. The notation $(\,)^o$ indicates the value of a quantity at the point O. Since the base vectors $\mathbf{G}_i^o$ are almost orthogonal unit vectors with errors of the order of small strains, a set of orthogonal unit vectors $\mathbf{i}_i^*$ satisfying

$$\mathbf{i}_i^* . \mathbf{i}_j^* = \delta_{ij} \tag{6}$$

and

$$\mathbf{G}_i^o . \mathbf{i}_j^* = \delta_{ij} + O(e) \tag{7}$$

is always present. One arbitrary set of such base vectors $\mathbf{i}_i^*$ satisfying the conditions given by Eqs. (6) and (7) is selected for each subdomain $V_{(m)}$. An asterisk in the superscript denotes a quantity defined in the local coordinate system and also with components decomposed by the base vectors $\mathbf{i}_i^*$, whereas the same symbol without an asterisk stands for components decomposed by the base vectors $\mathbf{i}_i$. The rigid body rotation of the subdomain $V_{(m)}$ is then represented by a matrix of direction cosines T_{ij}^o given by

$$T_{ij}^o = \mathbf{i}_i . \mathbf{i}_j^* \tag{8}$$

This leads to the following relationships

$$\mathbf{i}_i^* = T_{ji}^o \mathbf{i}_j \tag{9}$$

$$\mathbf{i}_i = T_{ij}^o \mathbf{i}_j^* \tag{10}$$

Taking the rigid body displacement into account, the final position vector $\mathbf{R}(\mathbf{x})$ of a point $\mathbf{x}$ in each subdomain $V_{(m)}$ can be expressed as the sum of the final position vector $(x_i^o + u_i^o)\,\mathbf{i}_i$ of the point O, the vector $(x_i - x_i^o)\,\mathbf{i}_i^*$ from O to this point after the rigid body rotation expressed by T_{ij}^o, and the displacement $\mathbf{u}^* = u_i^*(\mathbf{x})\,\mathbf{i}_i^*$ of the point from the position after the rigid body displacement. Therefore,

$$\mathbf{R}(\mathbf{x}) = (x_i^o + u_i^o)\,\mathbf{i}_i + \{(x_k - x_k^o) + u_k^*(\mathbf{x})\} T_{ik}^o\,\mathbf{i}_i \tag{11}$$

Let us define a local Cartesian coordinate system for each subdomain after the rigid body displacement with $\mathbf{i}_i^*$ as the base vectors. To stick to the total Lagrangian approach, the origin of each local coordinate system is so chosen that the local coordinates of a material point after the rigid body displacement are equal to the global Lagrangian coordinates x_i, which are defined in the initial state. With this definition, the derivatives with respect to the material coordinates defined before and after the rigid body displacement are identical and the notation $(\,)_{,i}$ stands for either of them. In view of Eqs. (1) and (11), the displacement components and their derivatives with respect to the coordinates x_i are obtained as

$$\begin{aligned} u_i(\mathbf{x}) = &-(x_i - x_i^o) + u_i^o \\ &+ \{(x_k - x_k^o) + u_k^*(\mathbf{x})\} T_{ik}^o \end{aligned} \tag{12}$$

$$u_{i,j}(\mathbf{x}) = -\delta_{ij} + \{\delta_{kj} + u_{k,j}^*(\mathbf{x})\} T_{ik}^o \tag{13}$$

Because of the orthogonal nature of the coordinate transformation matrix, we have

$$T_{ki}^o T_{kj}^o = \delta_{ij} \tag{14}$$

Using this fact, the inverses of Eqs. (12) and (13) can be expressed as

$$\begin{aligned} u_i^*(\mathbf{x}) = &-(x_i - x_i^o) \\ &+ [(x_k - x_k^o) + \{u_k(\mathbf{x}) - u_k^o\}] T_{ki}^o \end{aligned} \tag{15}$$

$$u_{i,j}^*(\mathbf{x}) = -\delta_{ij} + \{\delta_{kj} + u_{k,j}(\mathbf{x})\} T_{ki}^o \tag{16}$$

Substituting Eqs. (2) and (9) into Eq. (7) leads to

$$(\delta_{ki} + u_{k,i}^o) T_{kj}^o = \delta_{ij} + O(e) \tag{17}$$

In view of this equation, Eq. (16) gives

$$u_{i,j}^{o*} = O(e) \tag{18}$$

which shows that the displacement gradient $u_{i,j}^{o*} = u_{i,j}^*(\mathbf{x}^o)$ at the point O is of the order of small strains.

The quantities of the order of $u_{i,jk}^*$ at the point O is represented by k^o, i.e.,

$$k^o = O(u_{i,jk}^{o*}) \tag{19}$$

Further, defining the order of the dimensions of a subdomain by

$$l \equiv \max|x_i - x_i^o| \qquad x_i \in V_{(m)} \tag{20}$$

and noting the following relationship by the Taylor expansion

$$u^*_{i,j}(\mathbf{x}) = u^{o*}_{i,j} + u^{o*}_{i,jk}(x_k - x^o_k) + O\{(x_k - x^o_k)^2\} \quad (21)$$

the magnitude of the displacement gradient, in view of Eq. (18) and ignoring the terms of the second and higher orders, can be put in the form

$$u^*_{i,j}(\mathbf{x}) = O(e) + k^o l \quad (22)$$

If the dimensions of each subdomain are small enough so that the following condition is satisfied

$$k^o l = O(e) \quad (23)$$

Eq. (22) leads to

$$u^*_{i,j}(\mathbf{x}) = O(e) \quad (24)$$

Substituting Eqs. (10) and (13) into Eq. (2), the base vectors $\mathbf{G}_i$ can also be expressed in terms of the base vectors $\mathbf{i}^*_i$ of the local coordinate system and the displacement components u^*_i as

$$\mathbf{G}_i(x) = \{\delta_{ji} + u^*_{j,i}(\mathbf{x})\}\mathbf{i}^*_j \quad (25)$$

Substituting Eq. (25) into Eq. (3), the Green's strain tensor defined for the global coordinate system can be expressed in terms of the displacement components u^*_i decomposed by the local base vectors $\mathbf{i}^*_i$ as

$$e_{ij} = \frac{1}{2}(u^*_{i,j} + u^*_{j,i} + u^*_{k,i}\, u^*_{k,j}) \quad (26)$$

Equation (26) shows that the Green's strain tensor e_{ij} in the global coordinate system is equal to the Green's strain tensor e^*_{ij} defined in the local coordinate system. While $u_{i,j}$ is generally not a small quantity, Eq. (24) shows that, with a proper selection of $\mathbf{i}^*_i$ so as to satisfy Eqs. (6) and (7), the orders of magnitude of the terms $u^*_{i,j}$ and $u^*_{k,i}\, u^*_{k,j}$ are e and e^2, respectively. Hence, Eq. (26) can be written as

$$e_{ij} = e^*_{ij} = \{1 + O(e)\}\varepsilon^*_{ij} \quad (27)$$

where

$$\varepsilon^*_{ij} = \frac{1}{2}(u^*_{i,j} + u^*_{j,i}) \quad (28)$$

It is noted here that ε^*_{ij} is the small strain tensor defined in the local coordinate system with the base vectors $\mathbf{i}^*_i$. Thus, the Green's strain tensor $e_{ij} = e^*_{ij}$ is equal to the small strain tensor ε^*_{ij} defined in the local coordinate system within the error of the order of small strains. Such a relationship, however, does not hold between the Green's strain tensor and the small strain tensor $\varepsilon_{ij} = (u_{i,j} + u_{j,i})/2$ defined in the global coordinate system.

3. GOVERNING EQUATIONS

Let V and S^E be the volume and the external surface of an elastic body in the initial loading-free state. The governing differential equations in each of the subdomains $\{V_{(m)},\ m = 1, 2, \ldots, M\}$ of an elastic body are[14), 15)]

$$e_{ij} = \frac{1}{2}(u_{i,j} + u_{j,i} + u_{k,i}\, u_{k,j}) \quad (29)$$

$$\sigma_{ij} = E_{ijkl} e_{kl} \quad (30)$$

$$\{(\delta_{ij} + u_{i,j})\sigma_{kj}\}_{,k} + X_i = 0 \quad (31)$$

where σ_{ij} = second Piola-Kirchhoff stress tensor; X_i = body force per unit original volume decomposed by the global base vectors $\mathbf{i}_i$; and E_{ijkl} = tensor of elastic moduli. The boundary condition on the part of the external surface bounding the m-th subdomain, denoted by $S^E_{(m)}$, is given as either

$$[u_i]_{V_{(m)}} = [\overline{u}_i]_{S^E_{(m)}} \quad (32)$$

or

$$[(\delta_{ij} + u_{i,j})\sigma_{kj}\nu_k]_{V_{(m)}} = [\overline{F}_i]_{S^E_{(m)}} \quad (33)$$

where $\overline{u}_i$ = prescribed displacement; $\overline{F}_i$ = prescribed external force per unit area; and ν_i = direction cosines between the unit outward normal vector and the base vectors $\mathbf{i}_i$.

Internal surfaces between the subdomains are expressed by $\{S^I_{(n)},\ n = 1, 2, .., N\}$, where N is the total number of the internal surfaces. The boundary conditions on each internal surface $S^I_{(n)}$ between adjacent subdomains $V_{(m)}$ and $V_{(m')}$ are expressed as

$$[u_i]_{V_{(m)}} = [u_i]_{V_{(m')}} = [u_i]_{S^I_{(n)}} \quad (34)$$

and

$$[(\delta_{ij}+u_{i,j})\sigma_{kj}\nu_k]_{V_{(m)}} + [(\delta_{ij}+u_{i,j})\sigma_{kj}\nu_k]_{V_{(m')}} = [F_i]_{S^I_{(n)}} \tag{35}$$

where the right hand side of Eq. (35) is the surface force per unit area acting on the n-th internal surface.

Considering homogeneous and isotropic elastic materials, the elastic moduli are invariable with respect to a coordinate transformation. Hence, the stress tensor τ^*_{ij} of the small displacement theory in the local coordinate system is defined by utilizing the following constitutive relationship

$$\tau^*_{ij} = E_{ijkl}\varepsilon^*_{kl} \tag{36}$$

Substitution of Eqs. (27) and (36) into Eq. (30) yields

$$\sigma_{ij} = \{1+O(e)\}\tau^*_{ij} \tag{37}$$

Equation (37) implies that, within the range of small strains, the second Piola-Kirchhoff stress tensor can be approximated by the stress tensor τ^*_{ij} defined for the small displacement theory in the local coordinates, provided that a proper selection of $\mathbf{i}^*_i$ is made so as to satisfy Eqs. (6) and (7). Thus, Eq. (30) can be replaced by Eq. (36) in each subdomain because σ_{ij} and e_{ij} are equal to τ^*_{ij} and ε^*_{ij} respectively with errors of the order of small strains.

By the use of Eqs. (13), (26) and (30), Eq. (31) can be rewritten as

$$\frac{1}{2}T^o_{ih}\{(\delta_{hj}+u^*_{h,j})E_{kjlm}(u^*_{l,m}+u^*_{m,l} + u^*_{n,l}u^*_{n,m})\}_{,k} + X_i = 0 \tag{38}$$

Carrying out the differentiation with respect to x_i, the first term of Eq. (38) becomes

$$\begin{aligned}
&\tfrac{1}{2}T^o_{ih}\{(\delta_{hj}+u^*_{h,j})E_{kjlm}(u^*_{l,m}+u^*_{m,l} \\
&+u^*_{n,l}u^*_{n,m})\}_{,k} = \tfrac{1}{2}T^o_{ij}E_{kjlm}\{(u^*_{l,m}+u^*_{m,l})_{,k} \\
&+(u^*_{n,l}u^*_{n,mk}+u^*_{n,m}u^*_{n,lk})\} \\
&+\tfrac{1}{2}T^o_{ih}E_{kjlm}u^*_{h,j}\{(u^*_{l,m}+u^*_{m,l})_{,k} \\
&+(u^*_{n,l}u^*_{n,mk}+u^*_{n,m}u^*_{n,lk})\} \\
&+\tfrac{1}{2}T^o_{ih}E_{kjlm}u^*_{h,jk}(u^*_{l,m}+u^*_{m,l}+u^*_{n,l}u^*_{n,m})
\end{aligned} \tag{39}$$

In view of Eq. (24) and neglecting the terms of the order of the square of small strains, Eq. (39) leads to

$$\{(\delta_{ij}+u_{i,j})\sigma_{jk}\}_{,k} = \frac{1}{2}T^o_{ij}E_{kjlm}(u^*_{l,m}+u^*_{m,l})_{,k}\{1+O(e)\} \tag{40}$$

Further, using Eqs. (14), (28), (36) and (40) in Eq. (31), the equilibrium equation in the direction of $\mathbf{i}^*_i$ in a subdomain can be put in the form

$$\tau^*_{ki,k}\{1+O(e)\} + X^*_i = 0 \tag{41}$$

where $X^*_i = T^o_{ki}X_k$ = i-th component of the body force per unit original volume in the direction of $\mathbf{i}^*_i$. Equation (41) implies that the equilibrium equation of the finite displacement theory can be approximated within the error of the order of small strains by that of the small displacement theory when the rigid body displacement is properly separated in each subdomain. Under the same condition, it has been already shown that the strain-displacement relationship and the constitutive equation of the finite displacement theory can be approximated by Eqs. (27) and (36) respectively.

In view of Eqs. (12), (13), (14) and (37), the boundary conditions on the external surface $S^E_{(m)}$ as given by Eqs. (32) and (33) become

$$[-(x_i-x^o_i)+u^o_i+(x_k-x^o_k+u^*_k)T^o_{ik}]_{V_{(m)}} = [\bar{u}_i]_{S^E_{(m)}} \tag{42}$$

or

$$[\tau^*_{ji}\nu_j\{1+O(e)\}]_{V_{(m)}} = [\bar{F}^*_i]_{S^E_{(m)}} \tag{43}$$

where $\bar{F}^*_i = T^o_{ji}\bar{F}_j$.

Likewise, the continuity conditions on the internal surface $S^I_{(n)}$, given by Eqs. (34) and (35), can be expressed as

$$\begin{aligned}
&[-(x_i-x^o_i)+u^o_i+(x_k-x^o_k+u^*_k)T^o_{ik}]_{V_{(m)}} \\
&=[-(x_i-x^o_i)+u^o_i+(x_k-x^o_k+u^*_k)T^o_{ik}]_{V_{(m')}} \\
&=[u_i]_{S^I_{(n)}}
\end{aligned} \tag{44}$$

and

$$[T^o_{ij}\tau^*_{kj}\nu_k\{1+O(e)\}]_{V_{(m)}} + [T^o_{ij}\tau^*_{kj}\nu_k\{1+O(e)\}]_{V_{(m')}} = [F_i]_{S^I_{(n)}} \tag{45}$$

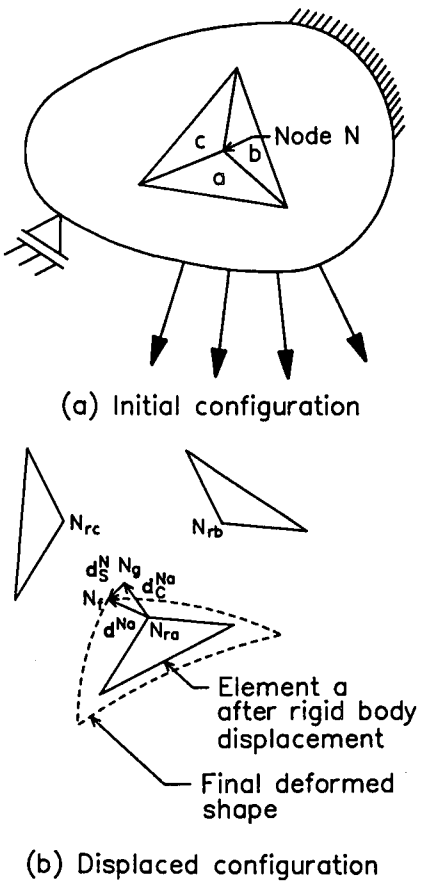

Fig. 1 Positions of a node

Summarizing the results, the governing differential equations of an elastic finite displacement problem can be replaced by those of the small displacement problem in each sufficiently small subdomain with errors of the order of small strains by separating the rigid body displacement so as to satisfy Eqs. (6), (7) and (23). The only differences compared with an elastic small displacement problem are the boundary conditions between subdomains. This is due to the fact that T_{ij}^o and u_i^o of adjacent subdomains are not identical because of the difference of their rigid body displacements. These differences were not stated in the past works.

4. SOLUTION PROCEDURE

(1) Basic solution technique by iteration

Since the rigid body rotation about an arbitrarily selected point O of each subdomain is generally not known, the direction cosines T_{ij}^o have to be guessed for each iterative step by an appropriate rule so as to satisfy Eqs. (6) and (7) as closely as possible. The rigid body displacements of the subdomains are not identical, and hence, a node shared by neighboring subdomains in the original state may be separated after the rigid body displacements. This is illustrated by a two-dimensional diagram in **Fig. 1**, where the positions of the same node N common to elements a, b and c are shown as N_{ra}, N_{rb} and N_{rc} after the rigid body displacements.

The equilibrium position of the node N is shown as N_f in **Fig. 1b**. Since the position N_f is unknown, it has to be guessed by an appropriate rule for each iterative step. The guessed position is shown as N_g, which is in general different from N_f.

The small generalized displacement vector including rotational components of the node N in the subdomain a from the position N_{ra} to the arbitrarily guessed position N_g is represented by $\mathbf{d}_C^N$ for a general subdomain, and by $\mathbf{d}_C^{Na}$ for the subdomain a. Similarly, the small generalized displacement vector from this guessed but known position N_g of the node N to the unknown exact position N_f is denoted by $\mathbf{d}_S^N$. The small generalized vector from N_{ra} to N_f is equal to the sum of $\mathbf{d}_C^{Na}$ and $\mathbf{d}_S^N$ and is denoted by $\mathbf{d}^N$ for a general subdomain, and by $\mathbf{d}^{Na}$ for the subdomain a. While $\mathbf{d}_C^N$ of a node N is different for each subdomain, $\mathbf{d}_S^N$ is common to all subdomains sharing the same node N. Hence, $\mathbf{d}_S^N$ can be used to superimpose the element stiffness equations to obtain the global stiffness equation.

The objective of the solution scheme is to improve the guessed nodal position N_g by iteration till it coincides with the true position N_f within a specified tolerance. Together with this process, the estimate of the rigid body displacement of each subdomain has also to be improved. On convergence, $\mathbf{d}_S^N$ becomes zero and $\mathbf{d}^N$ is equal to $\mathbf{d}_C^N$.

The final position $\mathbf{R}(\mathbf{x}^N)$ and directions of a node, which are known after the iteration has converged to the correct solution, can be written as

$$\mathbf{R}(\mathbf{x}^N) = (x_i^o + u_i^o)\,\mathbf{i}_i + \{(x_k^N - x_k^o) + u_k^{N*}(\mathbf{x}^N)\}\,T_{ik}^o\,\mathbf{i}_i \tag{46}$$

$$\theta_{ij}^N = \cos^{-1}(\mathbf{i}_i \cdot \mathbf{i}_j^N) = \cos^{-1} T_{ij}^N \tag{47}$$

with

$$T_{ij}^N = R_{jk}^N T_{ik}^o \tag{48}$$

and

$$[R_{ij}^N] = \begin{bmatrix} 1 & \phi_3^{N*} & -\phi_2^{N*} \\ -\phi_3^{N*} & 1 & \phi_1^{N*} \\ \phi_2^{N*} & -\phi_1^{N*} & 1 \end{bmatrix} \tag{49}$$

where $(\,)^N$ = value of a quantity at node N; θ_{ij}^N = angles between the global base vectors $\mathbf{i}_i$ and the nodal base vectors $\mathbf{i}_j^N$ at equilibrium state; and u_i^{N*} and ϕ_i^{N*} = translational and rotational components of $\mathbf{d}^N$ decomposed by the local base vectors $\mathbf{i}_i^*$.

(2) Stiffness equation

Let $\mathbf{D}_C^e$, $\mathbf{D}_S^e$ and $\mathbf{D}^e$ be the displacement vectors comprising the displacement vectors $\mathbf{d}_C^N$, $\mathbf{d}_S^N$ and $\mathbf{d}^N$ of all the nodes of an element. The displacement $\mathbf{D}^e$ of the element from the position and directions after the rigid body displacement is equal to $\mathbf{D}_S^e + \mathbf{D}_C^e$. Using the governing Eqs. (28), (36) and (41), the stiffness equation can be obtained in the local coordinate system by the finite element integration technique. The element stiffness equation so obtained can be expressed by transforming into global coordinate system as

$$\mathbf{T}^T\mathbf{K}^{e*}\mathbf{T}(\mathbf{D}_S^e + \mathbf{D}_C^e) - \mathbf{f}^{eo} = \mathbf{f}^e \tag{50}$$

where $\mathbf{T} = [T_{ij}^o]^T$, which is a function of the unknown rigid body rotation; $\mathbf{K}^{e*}$ = element stiffness matrix; $\mathbf{f}^e$ = nodal force vector of the element corresponding to $\mathbf{D}^e$; and $\mathbf{f}^{eo}$ = resultant nodal force vector due to the body forces. In the above equation, $\mathbf{D}_S^e$, $\mathbf{D}_C^e$, $\mathbf{f}^e$ and $\mathbf{f}^{eo}$ are vectors in the global coordinate system, while $\mathbf{K}^{e*}$ is written in the local coordinate system. When the small errors of the order of strains are completely neglected in the governing equations after the separation of the rigid body displacements, $\mathbf{K}^{e*}$ becomes equal to the elastic stiffness matrix $\mathbf{K}_E^{e*}$ of the familiar linear structural analyses. If the next higher order terms are retained, it becomes equal to the sum of the elastic and geometric stiffness matrices, i.e., $\mathbf{K}_E^{e*} + \mathbf{K}_G^{e*}$ [16].

Using the common nodal displacement vector $\mathbf{D}_S^e$ of all elements, the element stiffness equations can be superimposed, resulting in the following global equilibrium equation

$$\{\Sigma(\mathbf{T}^T\mathbf{K}^{e*}\mathbf{T})\}\mathbf{D}_S = \mathbf{f} + \Sigma\mathbf{f}^{eo} - \Sigma\{(\mathbf{T}^T\mathbf{K}^{e*}\mathbf{T})\mathbf{D}_C^e\} \tag{51}$$

where $\mathbf{D}_S$ = global displacement vector, of which $\mathbf{D}_S^e$ is a subvector; $\mathbf{f}$ = global external load vector corresponding to $\mathbf{D}_S$; and the summation sign symbolically represents the usual assembling procedure of the stiffness method.

(3) Iteration scheme

The estimates of the common nodal positions, N_g's, as well as the rigid body displacements of the elements for the first iterative step at a given load level can be obtained by appropriate extrapolations from the solutions for the preceding load levels. For the first load level, at which no preceding solution exists, the initial configuration could be used as the guess solution to begin the iterative procedure.

In the ν-th iterative step at a load level, $\mathbf{D}_C^{e,\nu}$ can be calculated from the guessed nodal positions and the guessed rigid body displacements. Substituting $\mathbf{D}_C^{e,\nu}$ into Eq. (51) and solving the linear system of equations, $\mathbf{D}_S^{\nu}$ is obtained. If $\mathbf{D}_S^{\nu}$ is not close to zero within a specified tolerance, the iterative procedure has to be continued to the $(\nu+1)$-th step. The nodal positions determined by adding $\mathbf{D}_C^{e,\nu} + \alpha\mathbf{D}_S^{e,\nu}$ to the configuration after the rigid body displacement in the ν-th step can be conveniently used as the new guessed common nodal points, N_g's, in the $(\nu+1)$-th step. Here, α is a positive factor normally taken as 1.0, but other values may be selected to improve the convergence of the iterative solution procedure. The rigid body displacement of each subdomain for the $(\nu+1)$-th iterative step can be decided by an appropriate prescribed rule, for example, by making the norm of $\mathbf{D}_C^{e,\nu+1}$ a minimum.

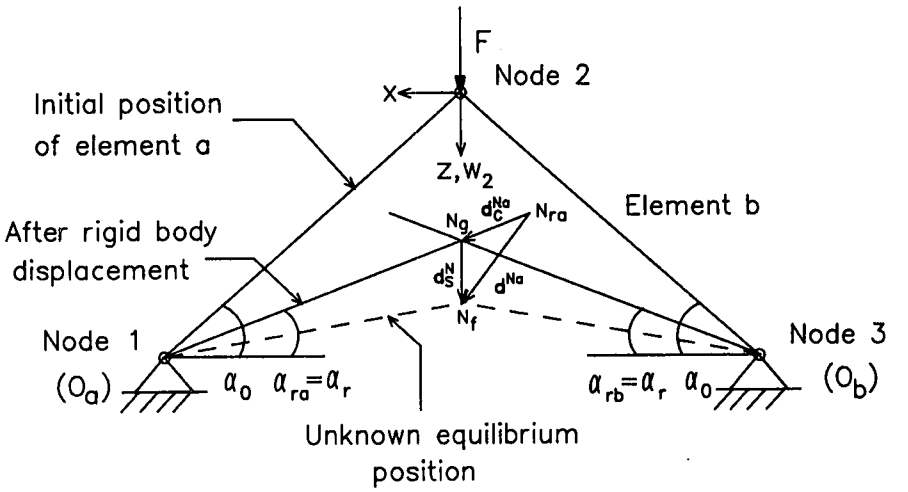

Fig. 2 Two-bar elastic truss

5. NUMERICAL EXAMPLES

Four simple numerical examples are presented to illustrate the theoretical concepts and to demonstrate the effectiveness of the solution procedure proposed in this paper. Although the theoretical development has been made for a three-dimensional solid, the governing equations of the structural elements used in the numerical examples can be easily obtained by imposing kinematic constraints on strain fields as explained in References 17 and 18.

(1) Two-bar truss

Consider an elastic two-bar truss under the action of a vertical load F at the top node, referred to as node 2, as shown in **Fig. 2**. The main objectives of this example are, firstly, to demonstrate numerically as well as theoretically that the inclusion or omission of the geometric stiffness matrix does not affect the final solution and, secondly, to explain the solution procedure for a simple case which does not require the use of a computer.

A global coordinate system (x, z) is defined with the origin at the initial unloaded position of node 2. The constitutive relation for a truss member in the displaced position is given by

$$N = \frac{EA(L_e - L)}{L} \tag{52}$$

where N = internal axial force; EA = axial rigidity; L_e = length in the equilibrium state; and L = initial length. Using Eq. (52) for both members, the elastic analytical relationship for the main equilibrium path, plotted in **Fig. 3** between the load F and the vertical displacement w_2 of node 2, is obtained as

$$F = 2EA\left(\sin\alpha_o - \frac{w_2}{L}\right)\times \left[\left\{1 - 2w_2 \sin\alpha_o / L + \left(w_2 / L\right)^2\right\}^{-0.5} - 1\right] \tag{53}$$

where α_o = angle between each truss member and the horizontal axis in the initial unloaded configuration.

The two elements are named a and b, and their rigid body displacements are referred to arbitrary points O_a and O_b, respectively, selected at the supports. Because of this, the rigid body translations of the elements always remain zero, and the rigid body displacements are completely specified by the angles α_{ra} and α_{rb} between the horizontal line and the axes of elements a and b, respectively.

Consider an iterative solution of this two-bar truss problem. For the main equilibrium path, the final position N_f of node 2 must be at $(0, z_{2f})$ by symmetry. Taking advantage of this symmetry, the guessed common point N_g is taken at $(0, z_{2g})$, and the same rigid body rotations are chosen for both elements a and b so that $\alpha_{ra} = \alpha_{rb} = \alpha_r$. To make the norm of $\mathbf{D}_C^e$ a minimum, each element should pass through the guessed common point, so that

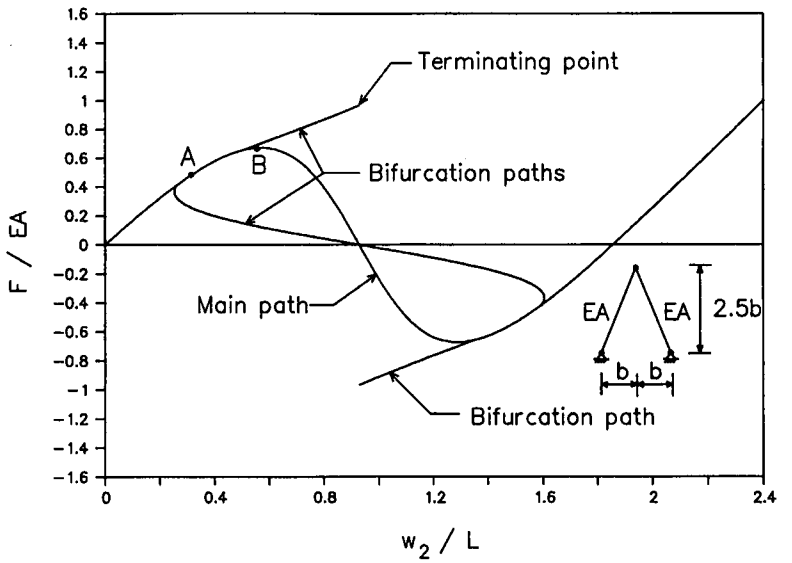

Fig. 3 Load-displacement curves (two-bar truss)

$$z_{2g} = L\sin\alpha_0 - L\cos\alpha_0\tan\alpha_r \tag{54}$$

The displacement vector $\mathbf{d}_C^N$ of node 2 of element a is given by

$$\mathbf{d}_C^{Na} = \begin{Bmatrix} u_{2c}^a \\ w_{2c}^a \end{Bmatrix} = \begin{Bmatrix} L\cos\alpha_r - L\cos\alpha_0 \\ L\sin\alpha_r - L\cos\alpha_0\tan\alpha_r \end{Bmatrix} \tag{55}$$

Designating the components of $\mathbf{d}_S^N$ at node 2 by $<u_{2S}\ w_{2S}>^T$ and imposing the kinematic boundary conditions at the support, the stiffness equation for element a corresponding to Eq. (50) using only the elastic stiffness matrix can be written as

$$\begin{bmatrix} \cos\alpha_r & \sin\alpha_r \\ -\sin\alpha_r & \cos\alpha_r \end{bmatrix}^T \begin{bmatrix} EA/L & 0 \\ 0 & 0 \end{bmatrix} \times \begin{bmatrix} \cos\alpha_r & \sin\alpha_r \\ -\sin\alpha_r & \cos\alpha_r \end{bmatrix} \left(\begin{Bmatrix} u_{2S} \\ w_{2S} \end{Bmatrix} + \begin{Bmatrix} u_{2c}^a \\ w_{2c}^a \end{Bmatrix} \right) = \begin{Bmatrix} f_{2x}^a \\ f_{2z}^a \end{Bmatrix} \tag{56}$$

Writing the element stiffness equation for element b and superimposing with Eq. (56), two simultaneous equations are obtained for two unknowns u_{2S} and w_{2S}. Since no horizontal force acts at node 2, $f_{2x}^a + f_{2x}^b = 0$. For this condition, it can be shown that $u_{2S} = 0$. Using this result leads to the following equilibrium equation in the vertical direction:

$$\begin{aligned} F &= f_{2z}^a + f_{2z}^b \\ &= 2EA(\sin\alpha_r - \cos\alpha_0\tan\alpha_r \\ &\quad + w_{2S}\sin^2\alpha_r / L) \end{aligned} \tag{57}$$

The criterion of convergence of the solution of the nonlinear equation (57) is $w_{2S} = 0$. Then, $\tan\alpha_r = \tan\alpha_0 - w_2\sec\alpha_0 / L$, and hence, Eq. (57) agrees exactly with the analytically obtained Eq. (53). This shows that the geometric stiffness matrix is not necessary to solve the finite displacement problem of this truss example when an iterative procedure converges.

The stiffness equation including the geometric stiffness matrix can be written in the same form as Eq. (56) except for the stiffness matrix, which is expressed as

$$\mathbf{K}^{e*} = \begin{bmatrix} EA/L & 0 \\ 0 & 0 \end{bmatrix} + \begin{bmatrix} 0 & 0 \\ 0 & N/L \end{bmatrix} \tag{58}$$

where $N = EA(\cos\alpha_0 / \cos\alpha_r - 1)$. Again, it can be easily shown that on convergence, the solution of the global stiffness equation agrees with the exact governing equation (53). This shows that the finite displacement solution for this truss example can also be obtained by including the geometric stiffness matrix.

For truss type structures, it is sufficient to treat each truss member as a subdomain. When the solution converges, the direction of the axis of a member after the rigid body displacement is the

Table 1 Number of iterations by various methods (two-bar truss)

Stiffness Matrix	Iteration scheme	At A F/EA=0.50 w_2/L=0.328	At B F/EA=0.67 w_2/L=0.547
$\mathbf{K}_E^{e*}$	Direct	13	98
	N-R	6	9
$\mathbf{K}_E^{e*}+\mathbf{K}_G^{e*}$	Direct	9	54

same as that in the equilibrium state. Because of this, the two normal components of the displacement vector $\mathbf{D}_C^{e*}=<u_1^{e*}\ w_1^{e*}\ u_2^{e*}\ w_2^{e*}>^T$, namely w_1^{e*} and w_2^{e*}, are equal to zero. Keeping in view that the geometric stiffness matrix for a truss member in the local coordinates is

$$\mathbf{K}_G^{e*}=\frac{N}{L}\begin{bmatrix}0&0&0&0\\0&1&0&-1\\0&0&0&0\\0&-1&0&1\end{bmatrix} \tag{59}$$

it is easily seen that $\mathbf{K}_G^{e*}\mathbf{D}_C^{e*}$ approaches zero on convergence. Hence, the omission of $\mathbf{K}_G^{e*}$ makes no difference on the final solution, provided that the procedure converges. In the present investigation, it is found that the solution does converge without $\mathbf{K}_G^{e*}$ for the entire range of the main equilibrium path. By an appropriate selection of N_g's and the rigid body displacements, the same is true for the entire range of the bifurcation paths obtained by Nishino and Hartono[19] up to the terminating points. However, the geometric stiffness matrix is needed to identify the bifurcation points and the initial guess solutions on the bifurcation paths. Both the main and bifurcation paths are shown in **Fig. 3**.

The stiffness equation, with or without $\mathbf{K}_G^{e*}$, is nonlinear due to the dependence of the transformation matrix on the unknown rigid body rotation. Hence, the solution can be obtained by either a direct iteration method using Eq. (51) or the Newton-Raphson (N-R) procedure, although convergence is not guaranteed for the former. The Newton-Raphson procedure was applied by solving Eq. (57) for α_r with $w_{2S}=0$. A comparison of the number of iterations required to obtain the solution by various methods with $\alpha_0=\tan^{-1}2.5$ is given in **Table 1** at a general point A, and at a point B close to a stationary point in the load-displacement curve as indicated in **Fig. 3**. The converged solutions obtained by all the methods agree with the analytical result of Eq. (53) within the specified tolerance of $|w_{2S}/L|\le 10^{-10}$. The load was applied in one step and the initial shape was used as the starting guess solution in all cases listed in **Table 1**. It is seen that, the Newton-Raphson method has the fastest convergence rate even though only the elastic stiffness matrix is used. However, the N-R procedure, as used in this simple example, cannot be applied so easily in a general case.

For the purpose of tracing the equilibrium path completely, as shown in **Fig. 3**, the load was applied in steps and the arc length control method[20)-22)] was utilized.

(2) Cantilever beam under axial load

An in-plane cantilever beam subjected to an axial end loading is considered as the second example. The objective of this example is to show that the accuracy of the result for a given element size when the geometric stiffness matrix is included may be better or worse than when it is omitted, depending on the location on the equilibrium path. Further, it is aimed to show both numerically and analytically that the effect of the geometric stiffness matrix diminishes with decreasing element size.

The non-dimensionalized vertical displacement w/L at the tip is plotted in **Fig. 4** against the normalized load F/F_{cr}, where F_{cr} is the Euler buckling load. A small transverse load $F_{dist}=0.0005F_{cr}$ was applied at the free end to disturb the beam from the possible straight unstable equilibrium configuration. The finite displacement behavior could be traced using either $\mathbf{K}_E^{e*}$ or $\mathbf{K}_E^{e*}+\mathbf{K}_G^{e*}$ for the entire range shown in **Fig. 4**. The results using one, two and sixteen two-dimensional beam elements are shown. The classical elastica solution based on the assumption of zero axial strain is also given for comparison. **Figure 5** shows errors in the calculated loads with and without $\mathbf{K}_G^{e*}$ at $w/L=0.4$ and 0.8.

In a single element model, a sharp increase of the lateral displacement, which corresponds to the buckling behavior, is obtained at a load about 20% higher than the Euler load when only $\mathbf{K}_E^{e*}$ is used. With a decreasing element length, this load tends to approach the theoretically correct value and the equilibrium path also approaches the elastica solution curve. When $\mathbf{K}_G^{e*}$

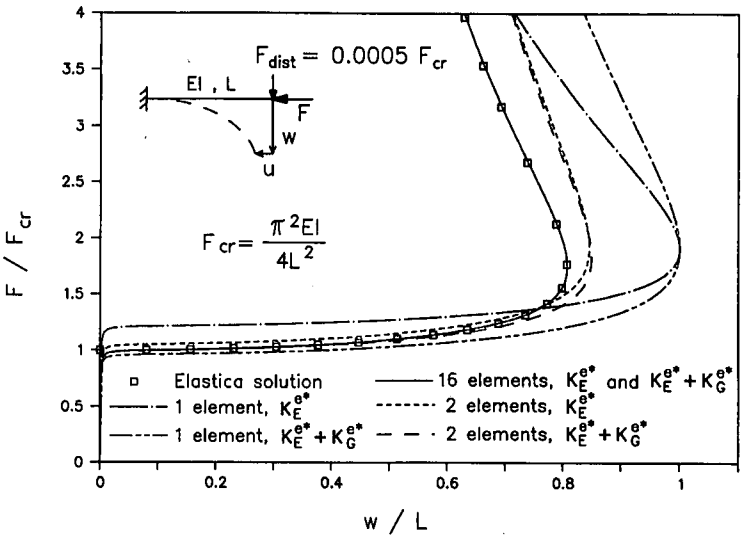

Fig. 4 Load-displacement curves (cantilever beam)

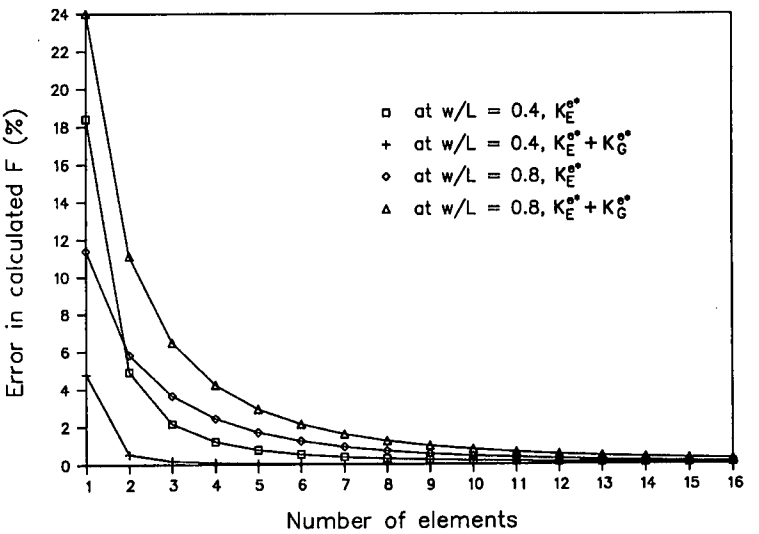

Fig. 5 Errors in calculated loads (cantilever beam)

is added, the buckling behavior starts at a value closer to the theoretical value. The accuracy of the solution in the post-buckling range, however, is not always better with $\mathbf{K}_E^{e*} + \mathbf{K}_G^{e*}$ than with $\mathbf{K}_E^{e*}$ alone, as can be seen in **Figs. 4 and 5**.

A relatively large number of iterations is necessary to obtain the solution points in the neighborhood of the Euler buckling load, especially when only $\mathbf{K}_E^{e*}$ is being used. On the other hand, the solution for a specified load anywhere in the post-buckling range can be obtained by a one-load-step analysis using $\mathbf{K}_E^{e*}$ alone. For instance, such an analysis with a sixteen-element model converges in 34 iterations for $F / F_{cr} = 1.5$ with a lateral disturbing force of $F_{dist} = 0.0005 F_{cr}$ within a tolerance of 10^{-10} for all displacements $(u / L, w / L, \theta)$. When $\mathbf{K}_G^{e*}$ is also included, however, the same analysis converges to a wrong configuration of the type noted by Cook[9]. Thus, it is always necessary to use several load steps with a closer interval in the region of the critical load to get the correct result in the post-buckling range when $\mathbf{K}_E^{e*} + \mathbf{K}_G^{e*}$ is used.

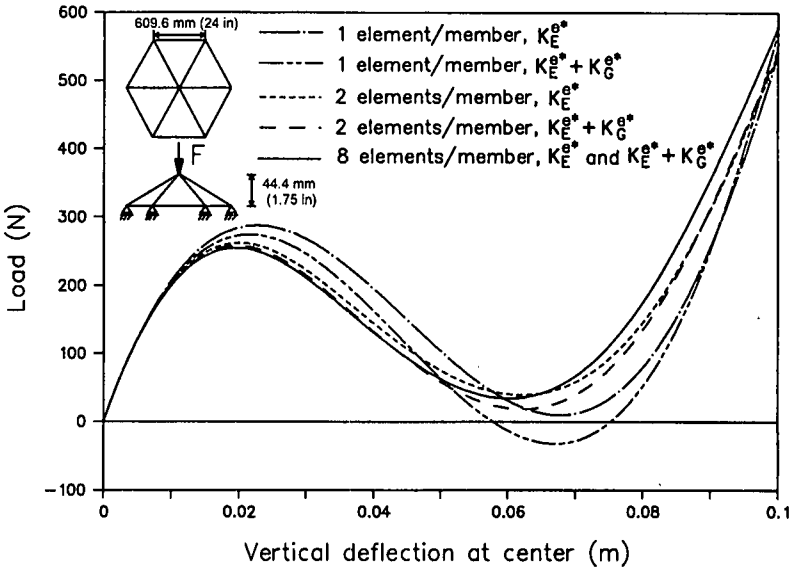

Fig. 6 Load-displacement curves (twelve-member hexagonal frame)

The well-known stiffness matrix for a two-dimensional beam element can be written in the form[23]

$$\mathbf{K}_E^{e*} + \mathbf{K}_G^{e*} = \mathbf{K}_1 + (NL^2 / EI)\mathbf{K}_2 \qquad (60)$$

where $\mathbf{K}_1$ and $\mathbf{K}_2$ are the non-dimensional coefficients of the elastic and geometric stiffness matrices, respectively, when non-dimensional displacement and force vectors are used. Equation (60) shows that, as the element size L is made shorter, the contribution of the geometric stiffness to the total stiffness matrix tends to zero. This observation is confirmed by the numerical results shown in **Fig. 4**. It also agrees with the former theoretical sections of this paper, where it was shown that the effects of the nonlinear terms can be reduced in the governing equations by making the size of the subdomains smaller.

(3) Twelve-member hexagonal frame

The behavior of a twelve-member hexagonal space frame under a vertical load at the center, as shown in **Fig. 6**, is studied by both taking into account and neglecting the geometric stiffness matrix. The objective of this example is to show that the proposed procedure can handle a problem in which finite rotations occur in three-dimensional space. This frame was studied experimentally by Griggs[24] using a plexiglas model test and analyzed by Chu and Rampetsreiter[25] by the constant load method using the stiffness coefficients of Renton[26]. All the members have a solid square cross-section with each side equal to 17.86 mm (0.703 in), and the Young's and shear moduli are equal to 3032 MPa (439.8 ksi) and 1096 MPa (159 ksi), respectively. The vertical displacement at the center calculated by the proposed method is plotted against the load in **Fig. 6**. The results obtained by using one, two and eight twelve-degree-of-freedom three-dimensional beam elements per member are shown. **Table 2** shows the computed values of the load at the maximum stationary point for a variety of cases.

Table 2 Load in N at the maximum stationary point (twelve-member hexagonal frame)

Stiffness Matrix	No. of elements per member			
	1	2	4	8
$\mathbf{K}_E^{e*}$	288.0	262.6	257.6	255.7
$\mathbf{K}_E^{e*} + \mathbf{K}_G^{e*}$	274.7	258.3	255.8	255.2

Once again, it is demonstrated that the results with and without $\mathbf{K}_G^{e*}$ converge to the same value with a decreasing element length. This value is close to Griggs' experimental measurement of 251.6 N (56.5 lb)[24]. For comparison, it is noted here that Chu and Rampetsreiter calculated this load as 270.3 N (60.7 lb)[25].

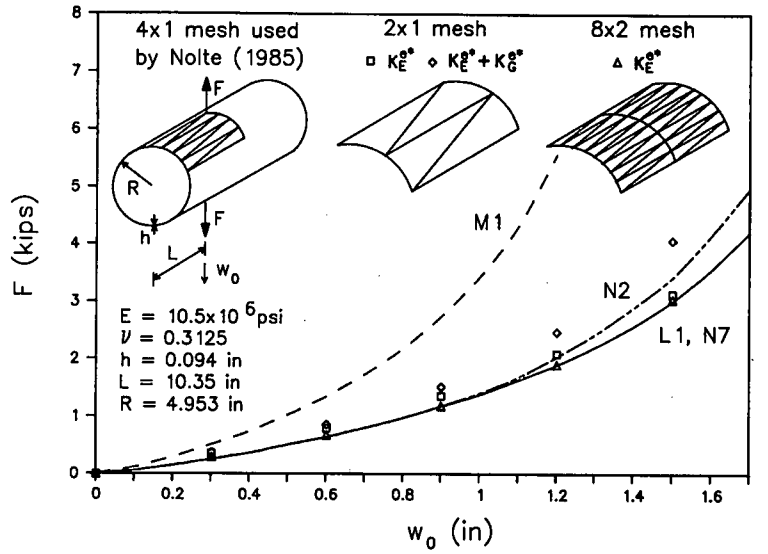

Fig. 7 Load-displacement curves of cylindrical shell (1 in = 0.0254 m; 1 kip = 4.45 kN; 1 psi = 6.89 kPa)

(4) Cylindrical shell under two concentrated loads

The proposed procedure can also be used to solve shell problems involving large rotations. As an example, a cylindrical shell free at both ends and subjected to two concentrated loads forming a self-equilibrium state as shown in **Fig. 7** was solved. Also shown in the same figure are the dimensions, the modulus of elasticity and the Poisson's ratio. This shell was selected since a number of methods were tried in the literature to solve this problem. The solutions were significantly different depending on the treatment of the finite rotations.

Figure 7 shows a number of solution curves given by Nolte[27] using several theories and the results obtained by the proposed method. *M1* denotes the results based on the classical shell theories by Donnell[28] and Vlasov[29], modified by the decomposition of strains and rotations to the extent that moderate rotations can be treated. *N2* and *N7* were calculated using the modified shell theories by Kratzig et al.[30] and Harte[31], respectively. These theories were derived with the same decomposition but on a priori different assumptions, so that large rotations could be handled. *L1* shows the results computed employing the theory by Nolte and Stumpf[32] using the Kirchhoff-Love constraints, expanded into series with respect to the linearized parameters at the deformed state and truncated within the desired accuracy, combined with the polar decomposition. According to Nolte[27], *L1* is based on the simplified theory with the assumption that rotations about the tangents to the middle surface may be large while those about the normals remain small. He claims that this simplified theory yields results which are in full agreement with those computed by the more complicated version *N7*. This theory, however, is still very complicated compared to that used for the proposed procedure in this paper.

The numerical results of both *L1* and the proposed procedure were computed with one eighth of the cylinder taking advantage of symmetry. *L1* was obtained with eight condensed high-precision triangular finite elements as shown in **Fig. 7**. The triangular element used quintic polynomial shape functions for all displacement components and an exact geometrical description in 21 Gauss integration points, resulting in 54 degrees of freedom for an element[27].

The simplest available elastic and geometric stiffness matrices for a triangular plate element were used for solving this problem by the proposed procedure. For the derivation of the elastic stiffness matrix, a linear interpolation function was used for the in-plane displacements, and a complete cubic polynomial and three sub-elements were used for bending to obtain compatible displacement fields between the elements[33]. The geometric stiffness matrix for

bending was derived using an incomplete cubic polynomial interpolation function without any sub-element for simplicity, resulting in incompatible displacement fields between elements[34]. There are five degrees of freedom per node in the local coordinate system of this triangular plate element giving a 15×15 stiffness matrix. The stiffness matrix has to be expanded to 18×18 by inserting an appropriate number of zeros before transforming to the global coordinates to account for the sixth degree of freedom consisting of the rotation about the axis normal to the plane of the element[4]. The use of different interpolation functions does not create any problem since the use of the geometric stiffness matrix changes only the rate of convergence in the proposed procedure, but its use is not essential as long as the iterative procedure converges.

The problem was solved with 2×1 and 8×2 meshes with 4 and 32 elements respectively as shown in **Fig. 7**. The computation was done with the elastic stiffness matrix only, and also the sum of the elastic and geometric stiffness matrices. For this particular example, the results with only the elastic stiffness matrix are more accurate than those with both the elastic and geometric stiffness matrices for the same mesh. To avoid the congestion of points, the results with 32 elements are shown in **Fig. 7** only for the case with the elastic stiffness matrix alone. The solution by the proposed procedure approaches the solution curves *N7* and *L1* as the element size is reduced. **Figure 7** shows that the results with 32 elements agree well with *N7* and *L1*.

This example shows that the solution of this problem by the proposed procedure agrees with what are believed to be the most accurate solutions obtained using the complicated shell formulations in the literature. The fact that accurate solutions are obtained with the elastic stiffness matrix alone clearly indicates the inherent simplicity of the proposed procedure. This corresponds to the use of only the classical small-displacement plate theory, which is far less complicated than even the simplest nonlinear shell theories, such as those given by Donnell[28] and Vlasov[29]. **Figure 7** shows that the solution curve *M1* obtained by using the latter theories is obviously erroneous.

6. SUMMARY AND CONCLUSIONS

It has been shown that the governing nonlinear differential equations of a finite-displacement problem of a solid can be reduced to pseudo-linear equations with errors of the order of strains. This can be achieved by separating the rigid body components from the displacement fields of small enough subdomains. The nonlinearity is hidden in the transformation matrix of the pseudo-linear equations. As the rigid body displacements of adjacent subdomains are different, additional internal boundary conditions must be imposed between adjacent subdomains.

Based on the theoretical development, it is inferred that correct solutions of finite-displacement small-strain problems can be obtained with the help of the small displacement theory alone when the rigid body displacements are properly separated. In other words, a finite-displacement problem can be solved using only the linear elastic stiffness matrix of the small displacement theory. The errors due to the omission of the higher order terms, such as the geometric stiffness matrix, can be made negligible by reducing the element size. Unlike the geometric stiffness matrix, the elastic stiffness matrix is independent of the stress state and needs to be evaluated only once during an analysis.

A rigorous and straightforward theoretical formulation has been presented to support the proposed solution technique based on the concept of removal of finite rigid body displacements. The simplicity of the formulation is due to the fact that it has been developed for a general three-dimensional solid unlike other similar works, in which rigid body displacements were separated from the governing equations of structural elements. The theoretical development of this paper, however, is equally applicable to structural members like beams, plates, etc. because the governing equations of the structural members can always be reduced from those of a solid by introducing additional kinematic constraints on strain fields[17), 18].

Several numerical examples are presented to demonstrate the effectiveness of the proposed solution procedure.

The authors believe that the theoretical explanation given in this paper is clearer and simpler than that of any other finite displacement formulation in the literature. Moreover, the present formulation is based on the total Lagrangian

governing equations and should be distinguished from the updated Lagrangian formulation.

REFERENCES

1) Martin, H.C.: On the derivation of stiffness matrices for the analysis of large deflection and stability problems, *Proc. of the First Air Force Conf. on Matrix Methods in Struct. Mech.*, AFFDL-TR-6680, Nov. 1965.
2) Mallett, R.H. and Marcal R.V.: Finite element analysis of nonlinear structures, *J. Struct. Div.*, ASCE, Vol. 94(ST9), pp. 2081-2105, 1968.
3) Bathe, K.-J., Ramm, E. and Wilson, E.L.: Finite element formulations for large deformation dynamic analysis, *Int. J. Num. Meth. Eng.*, Vol. 14, pp. 961-986, 1975.
4) Zienkiewicz, O.C.: *The Finite Element Method*, 3rd ed., McGraw-Hill Book Company (UK) Limited, 1977.
5) Yoshida, Y., Masuda, N. and Matsuda, T.: A discrete element approach to elastic-plastic large displacement analysis of thin shell structures, *Proc. of JSCE*, No. 288, pp. 41-55, August 1979 (in Japanese).
6) Obiya, H., Goto, S., Ijima, K. and Iguchi, S.: Large deformational analyses for plate and shell structures by the tangent stiffness method, *Proc. of JSCE*, No. 598, I-44, pp. 347-358, July 1998 (in Japanese).
7) Malvern, L.E.: *Introduction to the Mechanics of a Continuous Medium*, Prentice-Hall, New Jersey, 1969.
8) Maeda, Y. and Hayashi, M: Finite displacement analysis of space framed structures, *Proc. of JSCE*, No. 253, pp.13-27, September 1976 (in Japanese).
9) Cook, R.D.: *Concepts and Applications of Finite Element Analysis*, 2nd ed., John Wiley & Sons, New York, 1981.
10) Rankin, C.C. and Brogan, F.A.: An element independent corotational procedure for the treatment of large rotations, *J. Pressure Vessel Tech.*, ASME, Vol. 108, pp. 165-174, 1986.
11) Crisfield, M.A.: A consistent co-rotational formulation for non-linear, three-dimensional, beam-elements, *Comp. Meth. Appl. Mech. Engng.*, Vol. 81, pp. 131-150, 1990.
12) Goto, Y., Hasegawa, A. and Nishino, F.: Accuracy of finite displacement analysis of plane frames, *Proc. of JSCE*, No. 331, pp. 33-44, March 1983 (in Japanese).
13) Oran, C.: Tangent stiffness in space frames, *J. Struct. Div.*, ASCE, Vol. 99(ST6), pp. 987-1001, June 1973.
14) Fung, Y.C.: *Foundations of Solid Mechanics*, Prentice-Hall, New Jersey, 1965.
15) Washizu, K.: *Variational Methods in Elasticity and Plasticity*, 3rd ed., Pergamon Press, 1982.
16) Martin, H.C.: Finite elements and the analysis of geometrically nonlinear problems, *Recent Advances in Matrix Methods of Structural Analysis and Design*, Gallagher, R.H., Yamamoto, Y. and Oden, J.T. eds., UAH Press, The University of Alabama in Huntsville, Alabama, pp. 343-381, 1971.
17) Nishino, F. and Hasegawa, A.: Thin-walled elastic members, *J. of the Faculty of Engng.*, Vol. XXXV(2), The Univ. of Tokyo, pp. 109-190, 1979.
18) Nishino, F., Kasemset, C. and Lee, S.L.: Variational formulation of stability problems for thin-walled members, *Ingenieur-Archiv*, Vol. 43, pp. 58-68, 1973.
19) Nishino, F. and Hartono, W.: Influential mode of imperfection on carrying capacity of structures, *J. Engng. Mech.*, ASCE, Vol. 115(10), pp. 2150-2165, 1989.
20) Wempner, G.A.: Discrete approximations related to nonlinear theories of solids, *Int. J. Solids Struct.*, Vol. 7, pp. 1581-1599, 1971.
21) Riks, E.: An incremental approach to the solution of snapping and buckling problems, *Int. J. Solids Struct.*, Vol. 15, pp. 529-551, 1979.
22) Chaisomphob, T., Kanok-Nukulchai, W. and Nishino, F.: An automatic arc length control algorithm for tracing equilibrium paths of nonlinear structures, *Struct. Eng./Earthquake Eng.*, JSCE, Vol. 5(1), pp. 205s-208s, 1988.
23) Gallagher, R.H. and Padlog, J.: Discrete element approach to structural stability analysis, *AIAA J.*, Vol. 1(6), pp. 1437-1439, 1963.
24) Griggs, H.P.: *Experimental study of instability in elements of shallow space frames*, Research Report, Dept. of Civil Engng., MIT, Cambridge, Massachusetts, 1966.
25) Chu, K.-H. and Rampetsreiter, R.H.: Large deflection buckling of space frames, *J. Struct. Div.*, ASCE, Vol. 98(ST12), pp. 2701-2722, 1972.
26) Renton, J.D.: Stability of space frames by computer analysis, *J. Struct. Div.*, ASCE, Vol. 88(ST4), pp. 81-103, 1962.
27) Nolte, L.-P.: On the derivation and efficient computation of large rotation shell models, *Finite Rotations in Structural Mechanics*, Proc. Euromech Colloquium 197, Pietraszkiewicz, W. ed., Jablonna, Poland, Springer-Verlag, pp. 224-238, 1985.
28) Donnell, L.H.: *Stability of Thin-Walled Tubes under Torsion*, NACA TR 479, 1933.
29) Vlasov, V.Z.: *General Theory of Shells and Its Application in Engineering*, NASA TT F-99, 1964.
30) Kratzig, W.B., Basar, Y. and Wittek, U.: Nonlinear behaviour and elastic stability of shells, *Buckling of Shells*, Proc. of a State-of-the-Art Colloquium, Ramm, E. ed., Springer Verlag, 1982.
31) Harte, R.: *Doubly Curved Triangular Finite Elements for the Linear and Geometrically Nonlinear Analysis of General Shell Structures*, KIB-TWM 82-10, Ruhr-Univ. Bochum, 1982 (in German).
32) Nolte, L.-P., and Stumpf, H.: Energy-consistent large rotation shell theories in Lagrangian description, *Mech. Res. Comm.*, Vol. 10(4), pp. 213-221, 1983.
33) Clough, R.W. and Tocher, J.L.: Finite element stiffness matrices for analysis of plate bending, *Proc. of the First Conf. on Matrix Methods in Struct. Mech.*, AFFDL-TR-66-80, Wright-Patterson Air Force Base, Ohio, pp. 515-546, 1965.
34) Nath, B.: *Fundamentals of Finite Elements for Engineers*, The Athlone Press, London, 1974.

(Received September 10, 1999)

剛体変位の除去による有限変位微少ひずみ弾性問題の数値解法

西野文雄・Sujan MALLA・櫻井孝昌

剛体変位を適切に除去すれば，有限変位微少ひずみ問題は微少変位問題として扱うことができる．このためには固体を微少に分割し，分割されたの各要素から他の要素とは独立に剛体変位を除去しなければならない．本論文はこの考えに基づき，数値解を求める目的で，理論展開の中に物理的な考えを入れず，数学演算のみで，剛体変位の除去による基礎方程式の定式化を行ったものである．数学演算のみで定式化ができたという簡明性は，過去の剛体変位の除去手法による定式化が構造要素について行われたのに対し，定式化を３次元の固体について行ったことによる．